*Desalination and Water Treatment*
www.deswater.com

doi: 10.5004/dwt.2020.25404

185 (2020) 124–131
May

# Effect of the wall thickness of an overflow pipe on the short-circuit flow

Yung-Sheng Lai[a], Rome-Ming Wu[a,b,*]

[a]*Department of Chemical and Materials Engineering, Tamkang University, 151 Ying-chuan Road, Tamsui, Taipei County 25137, Taiwan, Tel. +886-2-2621-5656; Fax: +886-2-2620-9887; emails: jwu@mail.mcut.edu.tw (R.-M. Wu), yu999chia@mail.tku.edu.tw (Y.-S. Lai)*
[b]*Department of Safety, Health and Environmental Engineering, Ming Chi University of Technology, 84 Gong-Juan Rd., Taishan, New Taipei 243, Taiwan, ROC*

Received 5 January 2019; Accepted 25 December 2019

**ABSTRACT**

This study adopted FLUENT, a computational fluid dynamics software program, for the three-phase flow simulation of a hydrocyclone. The flow field and air-core of a hydrocyclone were simulated through the large eddy simulation methodology and volume of the fluid multiphase flow model. The Reynolds stress model was used as the coupled turbulent model. The particle flow was then simulated using a discrete phase model for examining the influence of the wall thickness of the hydrocyclone overflow pipe on the short-circuit flow and particle grade efficiency. The results revealed that an appropriate thickness of the overflow pipe wall should be selected to avoid short-circuit flow.

*Keywords:* Overflow; Thickness; Efficiency; Particle; CFD

## 1. Introduction

A hydrocyclone is a favored classification device for conducting solid separation [1]. Hydrocyclones are primarily applied in domains such as mineral processing [2], dewatering [3] (to a growing extent), environmental engineering [4], and water treatment [5–8]. With the development in science and technology, mathematical models based on computational fluid dynamics (CFD) have become highly desirable for solving flow fields in hydrocyclones [9].

Boysan et al. [10] adopted algebraic stress and random track models for the numerical calculation of two-phase turbulent flows within a hydrocyclone separator and predicted the fractional efficiency curve. Their calculation method provides a useful reference for the numerical simulation of a two-phase flow field of a hydrocyclone separator. Dyakowski and Williams [11] applied the Reynolds stress equation and the $k$–ε model as a solution and replaced the air column with a cylindrical bar. The calculation results of their study were similar to the experimental results. However, the algebraic expression of Reynolds stress in the calculation model must still be improved, and the model calculation is very time-consuming. Pericleous and Rhodes [12] were the first to successfully predict the flow field of a hydrocyclone separator with a diameter of 200 mm. They found that the higher the granular concentration, the higher was the valid viscosity at the wall and underflow sections. This higher concentration and viscosity intensified the interaction between continuous and discontinuous phases and complicated the fluid pattern.

The flow pattern complexity of a hydrocyclone separator, changes in the air core patterns, and CFD of unsteady flows were examined in [13]. An effective method to predict the air core is to use an empirical equation. Matvienko [14] compared different turbulent flow models and used them in a hydrocyclone separator simulation. Olson and Ommen [15] adopted CFD for determining the optimum design of a hydrocyclone separator and selected a multiphase flow

* Corresponding author.

model (algebraic mixture model), grain motion model, and turbulent flow model (Reynolds stress model (RSM)). The air core affects the flow split ratio and then the grade curve.

CFD investigations are also focused on the air core. Delgadillo and Rajamani [16] adopted a multiphase flow model (volume of fluid) for modeling the air core and compared the CFD results of three turbulent models—the large eddy simulation (LES) model, RSM, and RNG $k$–ε model—by conducting experiments. The results revealed that the RNG $k$–ε model could not form an air core, whereas the remaining two models produced an air core. Moreover, the results of the LES model were the closest to the experimental values, and this model could approximate the flow characteristics of the internal flow field of a hydrocyclone separator better than the other models could. However, the disadvantage of LES models is that these models can only be applied to dilute solutions. Delgadillo and Rajamani [17] provided a more detailed description of the advantages and disadvantages of applying LES models to hydrocyclone separators.

Considerable efforts have been made to develop efficient hydrocyclones with some new structures for changing the flow characteristics of conventional hydrocyclones. For example, a water-injected hydrocyclone [18] was designed to interrupt the boundary layer flow for reducing the fine particle content in the underflow. Mainza et al. [19] proposed a hydrocyclone with one underflow exit and two overflow exits. The main function of the dual vortex finders in a three-product cyclone is to prevent the short-circuiting of the coarse material in the overflow and to promote a preferential separation of the material moving to the inner and outer overflow streams.

The FLUENT software program (ANSYS Inc., Pennsylvania, USA) has been widely applied in many engineering fields, such as drying [20], drinking water treatments [21], filtration [22,23], and hydrocyclone separation [24,25]. The objectives of this study were to investigate the flow pattern by using the LES methodology and RSM turbulent model through FLUENT. Moreover, the influence of the wall thickness of the hydrocyclone overflow pipe on the short-circuit flow and particle grade efficiency was analyzed. Narasimha et al. [26] found that although LES is time-consuming, it provides the descriptions of a vortex structure and air core, which are similar to the descriptions presented in the experimental results. After obtaining a solution for the fluid flow, particulate flow simulation was conducted by numerically tracking the motion of the particles in a Lagrangian frame of reference by using a discrete phase model [27]. The effect of the thickness of an overflow pipe wall on separation was examined.

## 2. Numerical methods

### 2.1. Geometry and meshes

The geometry of the hydrocyclone is displayed in Fig. 1. The diameters of the feed, overflow, underflow, and hydrocyclone were 10, 15, 8, and 45 mm, respectively. The length of the cylindrical part of the hydrocyclone was 65 mm and that of the cone part was 75 mm. Thus, an overall cone angle of 14° was obtained. The number of hybrid mesh volumes used in this study was approximately 100,000 (Fig. 2).

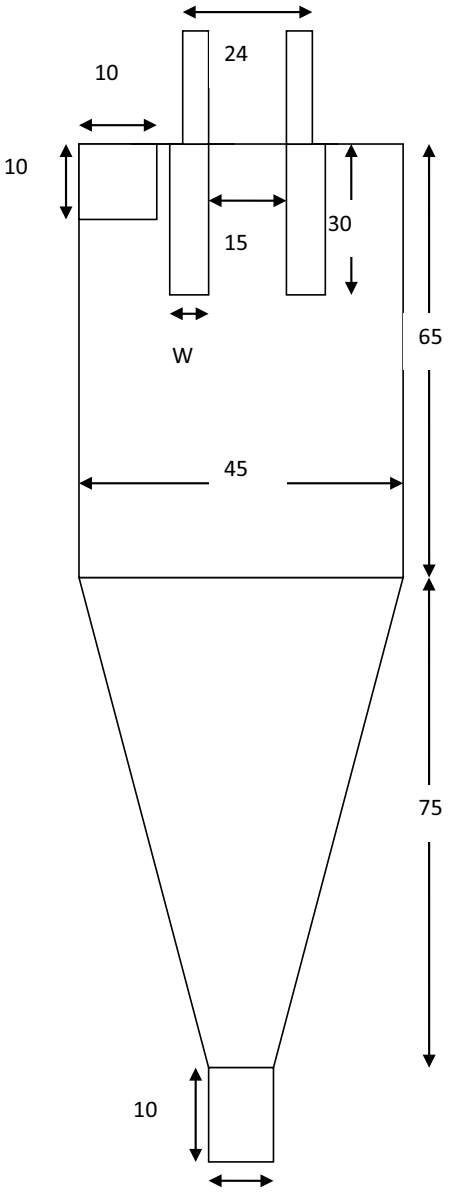


Fig. 1. The geometry of the hydrocyclone separator system used for CFD simulations.

### 2.2. Methodology

LES was conducted for simulating the flow patterns in the hydrocyclone separator system. The fluid velocity was decomposed using a filtering function into a larger-scale component and a residual component [28]. The filtering process effectively filtered out eddies whose values were smaller than the filter width or grid spacing used in the computations. A filtered variable, denoted by an overbar, was defined as follows:

$$\bar{\phi}(X) = \int_D \phi(X') G(X, X') dX' \quad (1)$$

where $D$ is the fluid domain and $G$ is the filter function that determines the scale of the resolved eddies. In the commercial

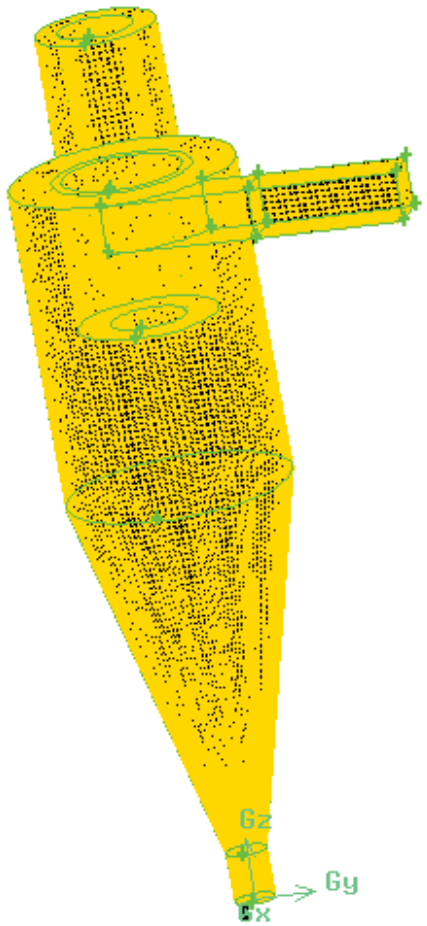


Fig. 2. Meshes of the hydrocyclone separator system used for CFD simulations.

CFD code FLUENT, the filtering operation is implicitly embedded within the finite-volume discretization process.

$$\bar{\phi}(X) = \frac{1}{V}\int_V \phi(X')\,dX', X' \in V \tag{2}$$

where $V$ is the volume of a computational cell. The filter function $G(X, X')$ can be expressed as follows:

$$G(X,X') = \begin{cases} \dfrac{1}{V}, X' \in V \\ 0, X' \quad \text{otherwise} \end{cases} \tag{3}$$

The following equations are obtained by filtering the Navier–Stokes equations:

$$\frac{\partial \rho}{\partial t} + \frac{\partial}{\partial x_i}\left(\rho \bar{u}_i\right) = 0 \tag{4}$$

$$\frac{\partial}{\partial t}\left(\rho \bar{u}_i\right) + \frac{\partial}{\partial x_j}\left(\rho \bar{u}_i \bar{u}_j\right) = \frac{\partial}{\partial x_j}\left(\mu \frac{\partial \sigma_{ij}}{\partial x_j}\right) - \frac{\partial \bar{p}}{\partial x_j} - \frac{\partial \tau_{ij}}{\partial x_j} \tag{5}$$

where $\sigma_{ij}$ is the stress tensor due to the molecular viscosity and is defined as follows:

$$\sigma_{ij} = \left[\mu\left(\frac{\partial \bar{u}_i}{\partial x_j} + \frac{\partial \bar{u}_j}{\partial x_i}\right)\right] - \frac{2}{3}\mu \frac{\partial \bar{u}_l}{\partial x_l}\delta_{ij} \tag{6}$$

Moreover, $\tau_{ij}$ is the subgrid-scale stress defined as follows:

$$\tau_{ij} \equiv \rho \bar{u}_i \bar{u}_j - \rho \bar{u}_i \bar{u}_j \tag{7}$$

### 2.3. Initial and boundary conditions

In this study, the inlet fluid was considered to move at a constant speed and the boundary condition was as follows:

$v$ = constant for the inlet pipe (8)

Moreover, the maximum inlet fluid velocity was 8.4 m/s. Starch powder particles with a density of 1,450 kg/m$^3$ were used as the simulated particles. Therefore, the flow Reynolds number based on the inlet diameter was approximately 44,000–1,20,000. The outlet fluid was moving under an absolute pressure of 1 atm; therefore, the gauge pressures for the underflow or overflow were zero. The boundary conditions were as follows:

$P = 0$ for the underflow (9)

$P = 0$ for the overflow (10)

No-slip boundary conditions were applied on all the hydrocyclone walls. A CFD program (FLUENT 6.1, ANSYS Inc., Pennsylvania, USA) was used to solve the governing equations (Eqs. (4)–(7)) with the associated initial and boundary condition equations (Eqs. (8)–(10)). This study adopted a pressure-staggered option scheme, which is a pressure interpolation scheme considered useful for predicting the high swirl flow characteristics inside the hydrocyclone body. Moreover, the SIMPLE algorithm was applied, which uses a combination of continuity and momentum equations to derive a pressure equation. This study then used the higher-order quadratic upwind interpolation convective kinematics spatial discretization scheme for the interpolation of field variables from the cell centers to the faces of the control volumes. The calculations were conducted for approximately 20,000-time steps, with a maximum relative error of $10^{-4}$ for fluid velocity evaluations at a time step of $10^{-4}$ s.

LES is a transient simulation that requires three dimensions and a fine grid. Therefore, grid independence studies were conducted. The results indicated that once the number of elements was halved and doubled, the solutions of the total separation efficiency had a maximum difference of 5.1% between the consecutive grids. The total separation efficiency $E_t$ was calculated using the following equation:

$$E_t = \frac{\left(G_u C_u\right)}{\left(G_e C_e\right)} \tag{11}$$

where $G_u$ and $G_e$ are the mass flows of the underflow and feed, respectively, and $C_u$ and $C_e$ are the solid weight concentrations of the underflow and feed, respectively. Our previous work can be referred to for the calculation method [25].

## 3. Results and discussion

### 3.1. Volume fraction of air, pressure, and velocity distribution

Figs. 3–5 present the air volume fraction, pressure, and absolute velocity distribution maps of the different hydrocyclones. In the simulation, the air-core formation was verified in four studied hydrocyclones with different overflow pipe thicknesses. When the inlet flow speed and overflow pipe diameter increased, the diameter of the air core increased. From a macroscopic viewpoint, Figs. 3–5 indicate that the wall thickness had no remarkable influence on the size and shape of the generated air core. Fig. 4 indicates that the static pressure was the largest at the wall and the lowest at the center, which is the air core area. Conversely, the absolute velocity was the lowest at the wall and the largest at the center (Fig. 5).

Fig. 6 displays the axial velocity distribution diagram presenting the X and Y cross-sectional views of a hydrocyclone with various overflow wall thicknesses. In the diagram, the colored section represents the axial velocity values of the upward flow in the *z*-direction, whereas the blank section represents the downward movement of the flow. As can be seen from the diagram, the hydrocyclone cannot simply be divided into the upward and downward speed regions. The division is a more complex situation that involves cross-doping.

### 3.2. Particle separation

Fig. 7 illustrates the trajectory of a particle released at different positions corresponding to Fig. 6. When the thickness of the overflow pipe wall was 1.5 mm, as at points A and B in Fig. 6a, the axial velocity closest to the overflow was upward. This suggested that upward particle transportation occurred in the fluid near the overflow pipe entrance, which led to short-circuit flow. Thus, the separation efficiency may deteriorate. Figs. 7a and b correspond to Fig. 6a at points A and B, respectively. The particles released at these two points exhibited outward overflow. Fig. 6 indicates that when the wall thickness is small, the liquid can easily move to the overflow end from the outside wall of the overflow pipe. This may cause large-size particles to flow out from the overflow end without separation, which is the short-circuit flow effect. A pipe with a wall thickness of 1.5 mm produces short-circuit flow; thus, the grade efficiency of small-size particles is considerably reduced at this thickness value.

The overflow pipe wall thickness was 2.5 mm, as at points C and D in Fig. 6b. The downward movement regions of fluid velocity near the entrance of the overflow were almost linked together. This caused particles to be carried away by the downward movement of the fluid upon reaching the underflow. Thus, superior separation efficiency was obtained. Figs. 7c and d correspond to Fig. 6b at points C and D, respectively. The particles released at these locations were carried away by the underflow.

Fig. 7e corresponds to Fig. 6c at point E. The thickness of the overflow pipe wall was 4.5 mm, as shown in Fig. 6c at point E. The downward movement regions of the fluid velocity were already linked together into one block. This caused particles to be carried away by the downward movement of the fluid upon reaching the underflow. Therefore, increased separation efficiency was attained. The particle released at point E was carried away by the underflow.

When the overflow pipe wall was 6.5 mm thick, as at point F in Fig. 6d, the overly thick overflow pipe wall caused the inside of the overflow pipe to be completely covered by upward movement regions of fluid velocity. This caused particles to be carried away by the fluid moving upward upon reaching the overflow. In this case, the separation efficiency

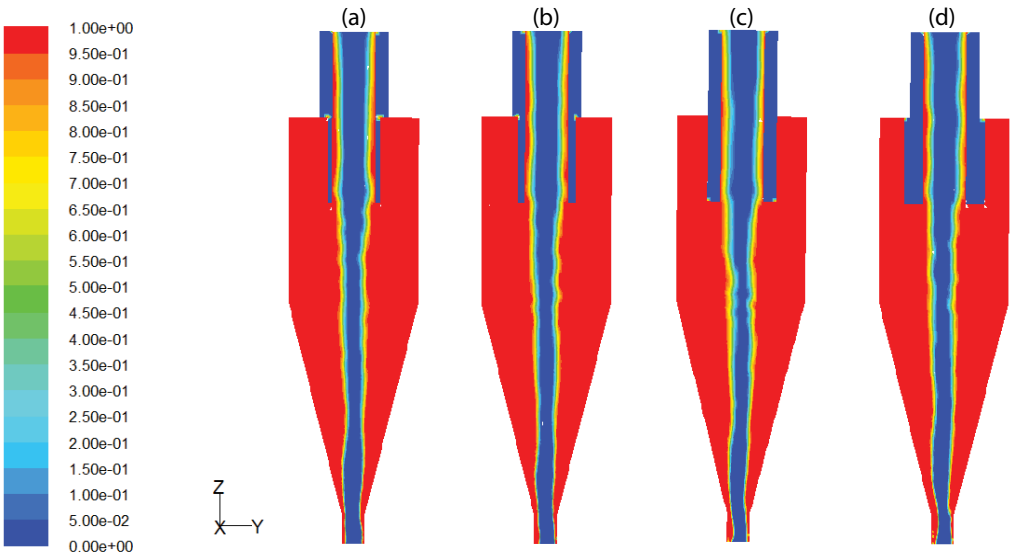


Fig. 3. Transient development of air core structure in the hydrocyclone separator system obtained from CFD simulations. (a) $W$ = 1.5 mm, (b) $W$ = 2.5 mm, (c) $W$ = 4.5 mm, and (d) $W$ = 6.5 mm.

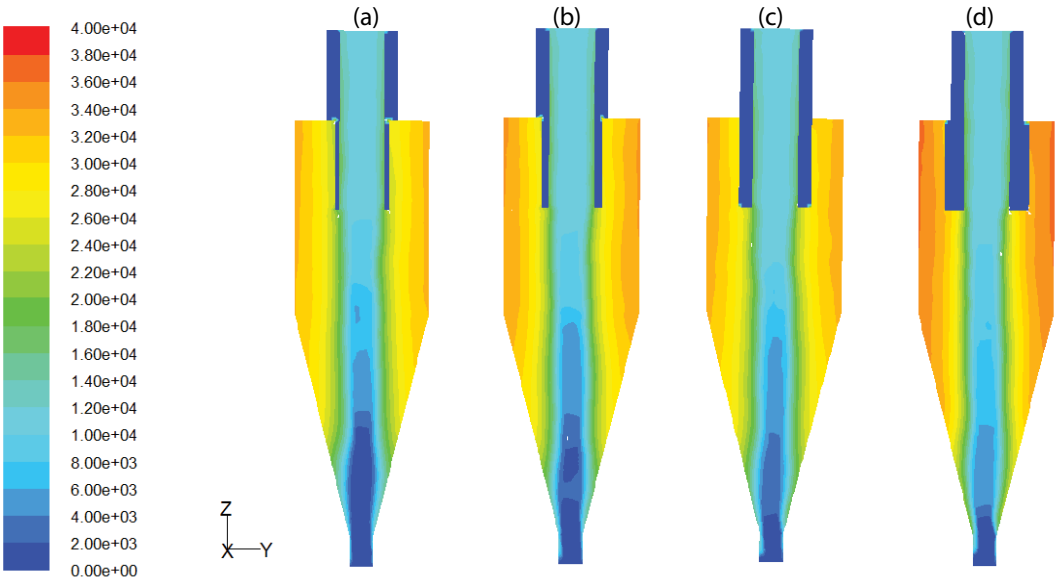


Fig. 4. Contour plots of pressure obtained from CFD simulations. (a) $W = 1.5$ mm, (b) $W = 2.5$ mm, (c) $W = 4.5$ mm, and (d)$W = 6.5$ mm.

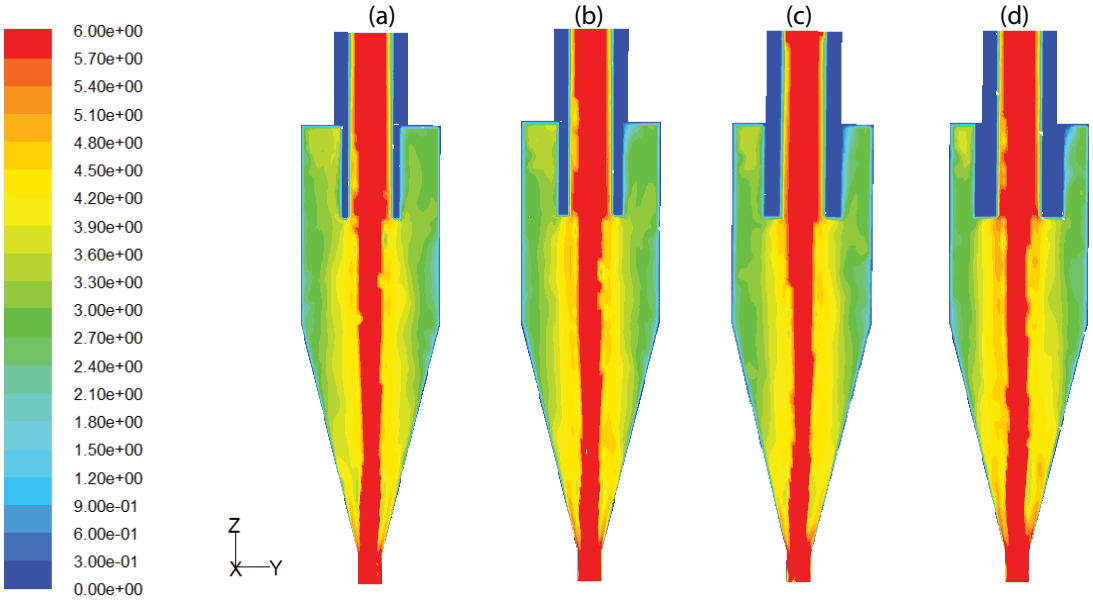


Fig. 5. Contour plots of tangential velocity obtained from CFD simulations. (a) $W = 1.5$ mm, (b) $W = 2.5$ mm, (c) $W = 4.5$ mm, and (d) $W = 6.5$ mm.

was not high. Fig. 7f corresponds to Fig. 6d at point F. The particle released at this location was carried away by the overflow.

Fig. 8 displays the grade efficiency diagram of different wall thicknesses of the pipe when the simulated flow split ratio was 0.85. The grade efficiency for small-size particles at a wall thickness of 4.5 mm was lower than that at a wall thickness of 2.5 mm. Moreover, the efficiency at a wall thickness of 1.5 mm was even lower than the aforementioned efficiencies. Thus, if the wall thickness is very small, the possibility of the occurrence of the short-circuit flow effect is high.

When the wall thickness was 6.5 mm, the grade separation curve was steep. A comparison between Fig. 6d suggests that small particles were carried away by the upward flow near the vicinity of the air column toward the entrance of the overflow, whereas large particles were carried away by the underflow when they were flung on the wall due to the centrifugal force. Therefore, the grade separation curve was steep. In summary, if a liquid has to be clarified or concentrated, the overflow pipe of a hydrocyclone should have a suitable wall thickness. The overflow pipe collects small-size particles, and the bottom pipe collects large-size particles.

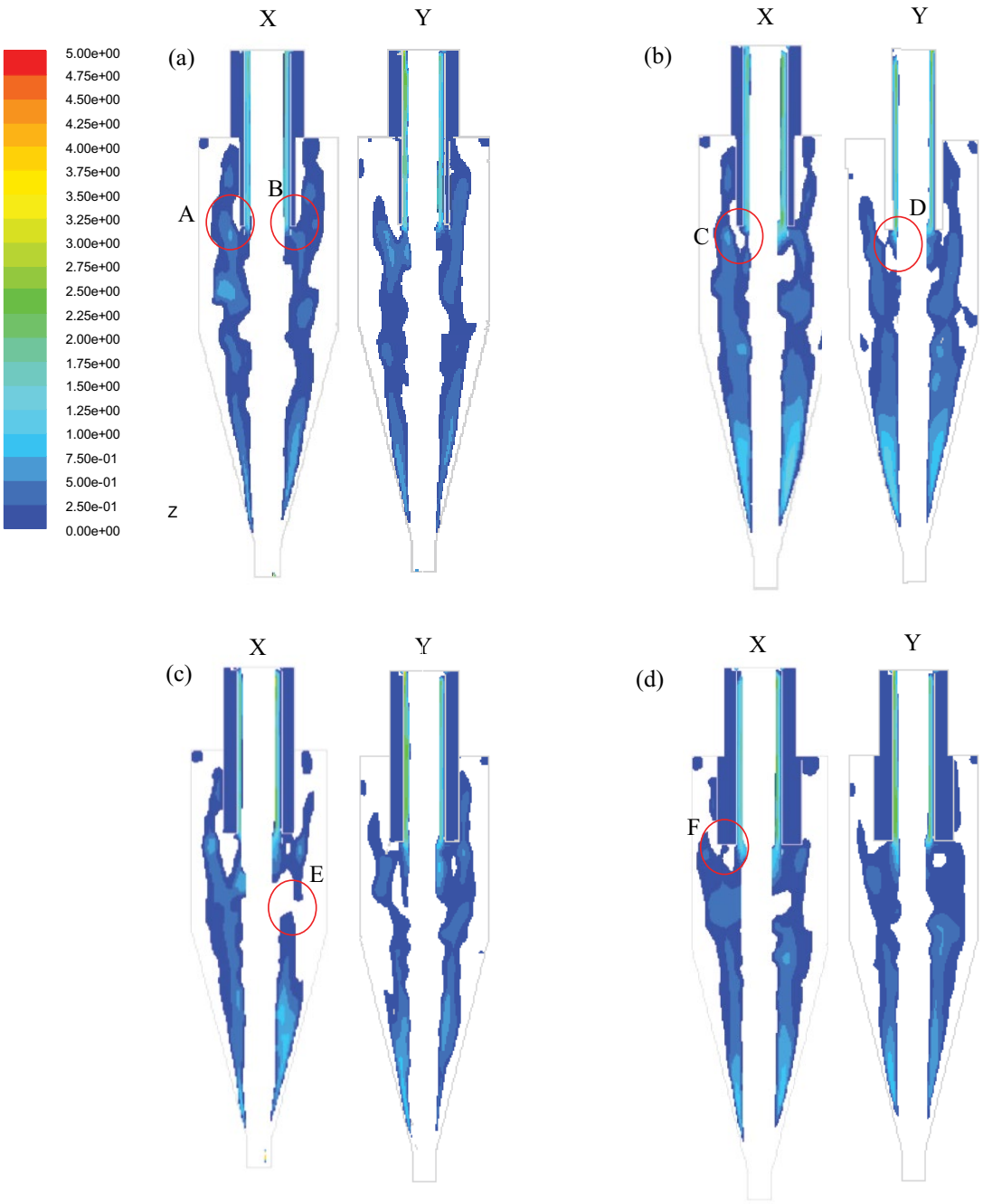


Fig. 6. Contour plots of vertical velocity obtained from As. (a) $W = 1.5$ mm, (b) $W = 2.5$ mm, (c) $W = 4.5$ mm, and (d) $W = 6.5$ mm.

Thus, a pipe with a thick wall should be selected for a hydrocyclone when separating small and large-size particles.

## 4. Conclusions

The simulation conducted in this study reveals that when an overflow wall is very thin or very thick, particles are carried away toward the overflow entrance. The overflow in the case of a very thin wall occurs due to a short-circuit flow, whereas the overflow in the case of a very thick wall occurs when the air column is covered by fluid that flows upward. When small particles are observed in this region due to an insufficient centrifugal force, the fluid carries the small particles away toward the overflow. The pipe wall thickness, which is crucial for the adjustment of short-circuit flow and the particle grade efficiency, can be used to achieve solid separation. If the overflow contains a supernatant liquid and the underflow contains a concentrated fluid, appropriate wall thickness should be used. If large-size particles must be separated from small-size particles, overflow pipes with thick walls are required. In practice, a rotating switch can be designed to alternate between various overflow pipe

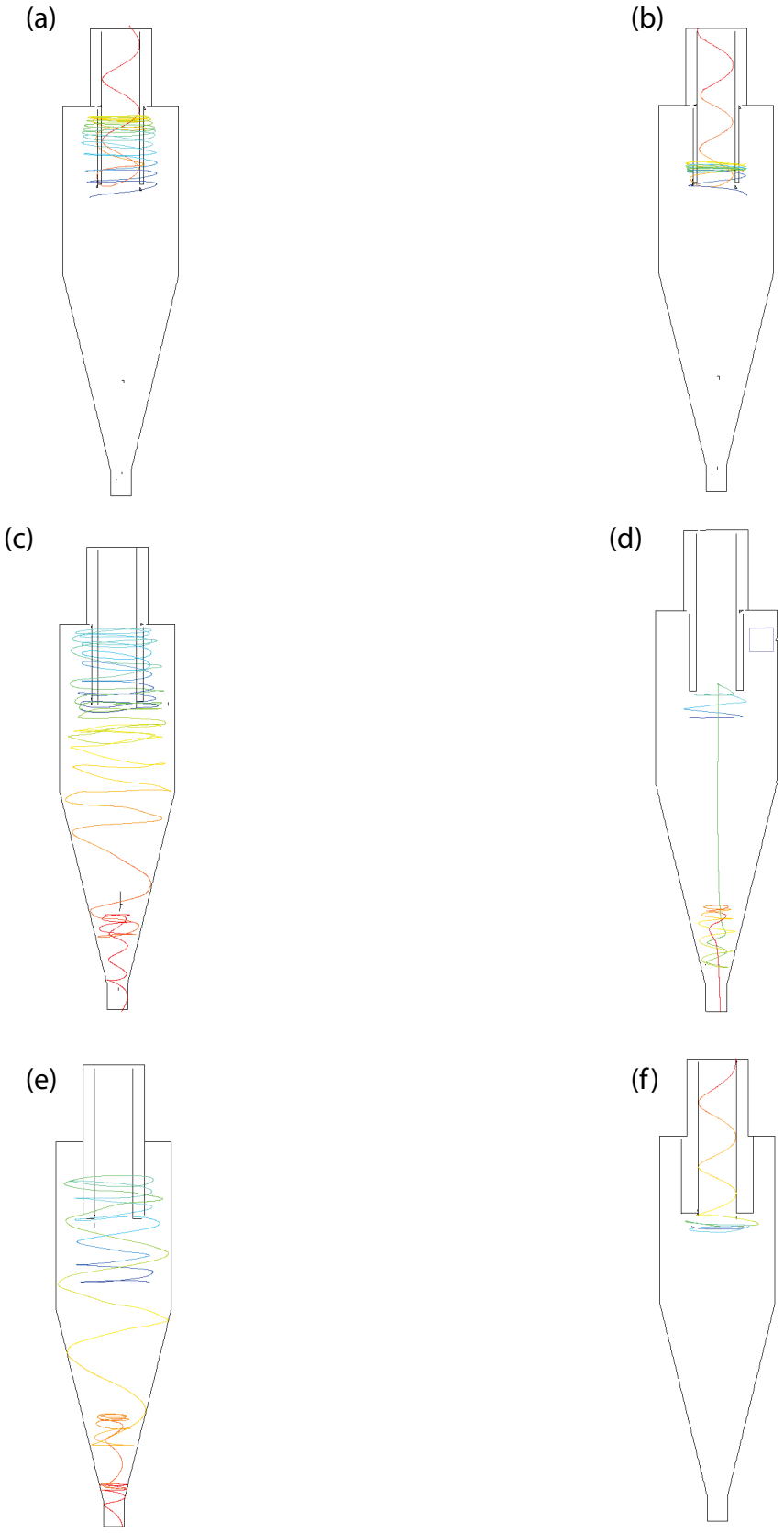


Fig. 7. Release single particle from different positions. (a) $W = 1.5$ mm, (b) $W = 1.5$ mm, (c) $W = 2.5$ mm, (d) $W = 2.5$ mm, (e) $W = 4.5$ mm, and (f) $W = 6.5$ mm.

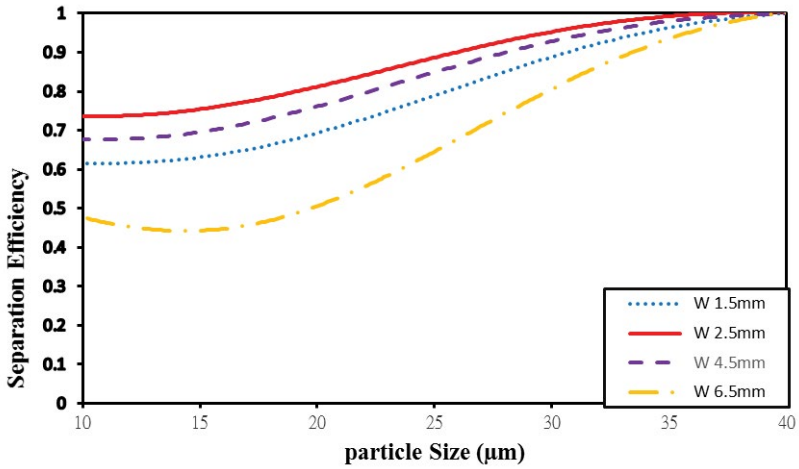


Fig. 8. Simulation of the grade efficiency curve diagram under different wall thicknesses. The flow split ratio is 0.85.

wall thicknesses for accommodating various operation requirements.

## Acknowledgments

The authors thank the National Science Council of the Republic of China, Taiwan, for financially supporting this study under contract number NSC 97-2221-E-032-030-MY3.

## References

[1] L.Y. Chu, W.M. Chen, Research on the motion of solid particles in a hydrocyclone, Sep. Sci. Technol., 28 (1993) 1875–1886.
[2] K.U. Bhaskar, B. Govindarajan, J.P. Barnwal, K.K. Rao, B.K. Gupta, T.C. Rao, Classification studies of lead–zinc ore fines using water-injection cyclone, Int. J. Miner. Process., 77 (2005) 80–94.
[3] S. Pasquier, J.J. Cilliers, Sub-micron particle dewatering using hydrocyclones, Chem. Eng. J., 80 (2000) 283–288.
[4] P. Romuald, J.H. Bokotko, J.D. Miller, Flue gas treatment for $SO_2$ removal with air-sparged hydrocyclone technology, Environ. Sci. Technol., 39 (2005) 1184–1189.
[5] W. Kim, M. Maeng, G. Myung, H. Lee, S. Dockko, Development of a hybrid treatment system for combined sewer overflows using a hydrocyclone and a dissolved air flotation system, Desal. Wat. Treat., 57 (2016) 7650–7658.
[6] J. Yu, Y. Kim, Hydrocyclone design and energy requirement for treating storm water runoff from bridge, Desal. Wat. Treat., 57 (2016) 629–635.
[7] J. Yu, H. Yu, Y. Chen, J. Cheng, Y. Kim, Post-treatment schemes of the outflow from hydrocyclone treating paved-road stormwater runoff, Desal. Wat. Treat., 51 (2013) 4028–4034.
[8] J.H. Son, M. Hong, H.C. Yoo, Y.I. Kim, H.D. Kim, J.T. Kim, A multihydrocyclone water pretreatment system to reduce suspended solids and the chemical oxygen demand, Desal. Wat. Treat., 57 (2016) 2996–3001.
[9] K.J. Hwang, W.H. Wu, S. Qian, Y. Nagase, CFD study on the effect of hydrocyclone structure on the separation efficiency of fine particles, Sep. Sci. Technol., 43 (2008) 3777–3797.
[10] F. Boysan, W.H. Ayers, J. Swithenbank, Fundamental mathematical modeling approach to cyclone design, Trans. Inst. Chem. Eng., 60 (1982) 222–230.
[11] T. Dyakowski, R.A. Williams, Modelling turbulent flow within a small-diameter hydrocyclone, Chem. Eng. Sci., 48 (1993) 1143–1152.
[12] K.A. Pericleous, N. Rhodes, The hydrocyclone classifier - a numerical approach, Int. J. Miner. Process., 17 (1986) 23–43.
[13] J.J. Derksen, H.E.A. Van Den Akker, Simulation of vortex core precession in a reverse-flow cyclone, AIChE J., 46 (2000) 1317–1331.
[14] O.V. Matvienko, Analysis of turbulence models and investigation of the structure of the flow in a hydrocyclone, J. Eng. Phys. Thermophys., 77 (2004) 316–323.
[15] T.J. Olson, V.R. Ommen, Optimizing hydrocyclone design using advanced CFD model, Miner. Eng., 17 (2004) 713–720.
[16] J.A. Delgadillo, R.K. Rajamani, A comparative study of three turbulence closure models for the hydrocyclone problem, Int. J. Miner. Process., 77 (2005) 217–230.
[17] J.A. Delgadillo, R.K. Rajamani, Hydrocyclone modeling: large eddy simulation CFD approach, Miner. Metall. Process, 22 (2005) 225–232.
[18] D.D. Patil, T.C. Rao, Classification evaluation of water injected hydrocyclone, Miner. Eng., 12 (1999) 1527–1532.
[19] A. Mainza, M.S. Powell, B. Knopjes, Differential classification of dense material in a three-product cyclone, Miner. Eng., 17 (2004) 573–579.
[20] A. Erriguible, P. Bernada, F. Couture, M.A. Roques, Modeling of heat and mass transfer at the boundary between a porous medium and its surroundings, Drying Technol., 23 (2005) 455–472.
[21] W.J. Yang, C.C. Wang, R.Y. Hsu, R.M. Wu, Two-phase flow simulation of reactor clarifiers, J. Chin. Inst. Chem. Eng., 39 (2008) 275–280.
[22] R.M. Wu, K.J. Li, Increasing filtrate flux of crossflow filtration with side stream, Sep. Sci. Technol., 45 (2010) 975–981.
[23] R.M. Wu, Y.J. Lin, Tubular membrane filtration with a side stream and its intermittent backwash operation, Sep. Sci. Technol., 47 (2012) 1689–1697.
[24] B. Wang, A.B. Yu, Numerical study of the gas-liquid-solid flow in hydrocyclones with different configuration of vortex finder, Chem. Eng. J., 135 (2008) 33–42.
[25] E.W.-C. Lim, Y.R. Chen, C.H. Wang, R.M. Wu, Experimental and computational studies of multiphase hydrodynamics in a hydrocyclone separator system, Chem. Eng. Sci., 65 (2010) 6415–6424.
[26] M. Narasimha, M. Brennan, P.N. Holtham, Large eddy simulation of hydrocyclone-prediction of air-core diameter and shape, Int. J. Miner. Process., 80 (2006) 1–14.
[27] M. Narasimha, R. Sripriya, P.K. Banerjee, CFD modeling of hydrocyclone-prediction of cut size, Int. J. Miner. Process., 75 (2005) 53–68.
[28] J.A. Delagadillo, R.K. Rajamani, Exploration of hydroclcylone designs using computational fluid dynamics, Int. J. Miner. Process., 84 (2007) 252–261.